MAGNETIC RESONANCE IN CHEMISTRY
Magn. Reson. Chem. 2006; **44**: S196–S205
Published online in Wiley InterScience (www.interscience.wiley.com). DOI: 10.1002/mrc.1818

Fast multidimensional NMR spectroscopy by spin-state selective off-resonance decoupling (SITAR)

Rochus Keller, Christy Rani R. Grace and Roland Riek*

Structural Biology Laboratory, The Salk Institute, La Jolla, CA, 92037, USA

Received 30 November 2005; Revised 23 January 2006; Accepted 28 February 2006

Spin-state selective off-resonance decoupling (SITAR) is applied to the amide proton-to-nitrogen-to-alpha-carbon correlation (HNCA) triple-resonance experiment by measuring the ^{15}N chemical shift during the acquisition simultaneously with the ^{1}H chemical shift. The simultaneous detection of both ^{1}H and ^{15}N chemical shifts in SITAR reduces the dimensionality of the HNCA-type experiment from three dimensions to two dimensions with a ^{15}N chemical shift resolution of ∼0.4 ppm. This enables the recording of triple-resonance experiments in several minutes. SITAR is furthermore applied to the amide proton-to-nitrogen-to-alpha-carbon-and-beta-carbon correlation (HNCACB) triple-resonance experiment and the ^{15}N-resolved [^{1}H,^{1}H]-nuclear Overhauser enhancement spectroscopy (NOESY) experiment with similar success.

The accompanied peak crowding and chemical shift degeneracy of the amide protons in the SITAR two-dimensional (2D) spectra, which are inherent properties of pseudo-dimensional experiments, are resolved by local correlation of the two sub-spectra. With this procedure a ^{13}C–^{1}H strip for each ^{15}N–^{1}H moiety is generated resulting in a three-dimensional (3D) strip list known from the conventional 3D spectra. The quality of the strip list in terms of peak crowding and chemical shift degeneracy is comparable to their corresponding 3D counterparts. An analysis-software within the CARA package is presented, which generates, visualizes and manages the SITAR spectra, the corresponding strip lists and the assignment process.

Supplementary electronic material for this paper is available in Wiley InterScience at http://www.interscience.wiley.com/jpages/0749-1581/suppmat/

KEYWORDS: fast multidimensional experiment; NMR; biological macromolecule; chemical shift-coded experiment; high-throughput resonance assignment; SITAR; spin state-selective off-resonance decoupling

INTRODUCTION

The recent development of the cryogenic probe increases the sensitivity of the nuclear magnetic resonance (NMR) spectrometers by a factor of ∼3–4 and concomitantly reduces the necessary measuring time by one order of magnitude. This achievement builds the basis for the so-called 'non-sensitivity-limited' data collection regime for well-behaving small and medium size proteins. In this regime, the minimum measurement time required is defined by the sampling rate of the multidimensional NMR experiment and not the sensitivity of the experiment. To circumvent the sampling problem, 'fast multidimensional NMR' methods have been recently proposed and applied to triple-resonance experiments, speeding up the measuring time by up to two orders of magnitude. These new schemes include G-matrix Fourier transform NMR spectroscopy (GFT-NMR), Hadamard spectroscopy and projection spectroscopy (for review see Ref. 1).[1] GFT-NMR spectroscopy[2] is a reduced-dimensionality approach, which is based on simultaneous evolution of two or more different chemical shifts reducing the dimensionality of a triple-resonance experiment by one or more. Kupce and Freeman applied Hadamard spectroscopy to the triple-resonance experiments HNCO and amide proton-to-nitrogen-to-carbonyl correlation (HNCA) and obtained the assignment of a small peptide after measuring only for a few minutes.[3] They also applied the three-dimensional (3D) projection spectroscopy to HNCA and HNCO experiments and obtained the spectrum of a protein after a few minutes of measuring time.[1]

Here, we are applying spin-state selective off-resonance decoupling (SITAR)[4] to obtain fast multidimensional NMR spectra. SITAR is based on the notion that chemical shift information can be extracted by off-resonance decoupling.[5] As we shall see, the use of SITAR for the detection of the ^{15}N chemical shift in HNCA-type triple-resonance experiments enables the measurement of a triple-resonance experiment in only several minutes. The chemical shift resolution is comparable to the conventional 3D counterpart. The crowding of the spectrum as well as the chemical shift degeneracy of the amide protons, which are inherent problems of pseudo-3D spectroscopy, are resolved by spin-state selection and an algorithm that uses local correlations

*Correspondence to: Roland Riek, Structural Biology Laboratory, The Salk Institute, 10010 N Torrey Pines Road, La Jolla, CA, 92037, USA. E-mail: riek@salk.edu

of the SITAR-spectra. Furthermore, a software module is developed for working efficiently with the SITAR-spectra in an easy manner. The proposed SITAR-based fast multidimensional NMR experiments are therefore very attractive for high-throughput approaches to small size proteins.

RESULTS

The concept of SITAR

We recently introduced an alternate technique for accurately monitoring the chemical shift in multidimensional NMR experiments, which is based on a combination of spin state selection and off-resonance (SITAR) decoupling.[4] By applying off-resonance decoupling on spin ^{15}N during acquisition of spin ^{1}H, the scalar coupling $^{1}J(^{1}\mathrm{H},^{15}\mathrm{N})$ between the spins is scaled and the residual scalar coupling turns out to be a function of the chemical shift of spin ^{15}N:[5]

$$\omega_{\mathrm{N}} = \omega_{\mathrm{cw}} \pm [{}^{\mathrm{R}}J(^{1}\mathrm{H},^{15}\mathrm{N})(\gamma_{\mathrm{N}}B_2/2\pi)/[{}^{1}J(^{1}\mathrm{H},^{15}\mathrm{N})^2 - {}^{R}J(^{1}\mathrm{H},^{15}\mathrm{N})^2]^{0.5}] \quad (1)$$

with the applied radio-frequency power for the decoupling $\gamma_{\mathrm{N}}B_2/2\pi$ at a ^{15}N frequency ω_{cw} and the actual $^{1}J(^{1}\mathrm{H},^{15}\mathrm{N}) = -92$ Hz. Thus, the chemical shift information of spin ^{15}N is indirectly retained, without an additional evolution period and the accompanying polarization transfer elements. The detection of the components of the doublet using spin state-selection enables an accurate measurement of the residual scalar coupling, which is then converted into a precise value for the chemical shift. The chemical shift resolution depends on the size and variation of the involved scalar coupling and the B1 inhomogeneity.[4] It is our finding that the small variation of $^{1}J(^{1}\mathrm{H},^{15}\mathrm{N})$ and the use of a state-of-the-art probe head can yield ^{15}N-chemical shift with a precision of ~0.1 ppm.[4] The spin state-selection yields two sub-spectra comprising either one of the two components of the doublet $I^{-}_{24} = \omega(^{1}\mathrm{H}) + {}^{R}J(^{15}\mathrm{N},^{1}\mathrm{H})$ or $I^{-}_{13} = \omega(^{1}\mathrm{H}) - {}^{R}J(^{15}\mathrm{N},^{1}\mathrm{H})$. Hence, the spin state-selection is avoiding the overlap problems that arise from off-resonance decoupling.

In general, SITAR can be incorporated into any pulse sequence. Here, the concept of SITAR is applied to fast multidimensional triple-resonance experiments and the ^{15}N-resolved $[^{1}\mathrm{H},^{1}\mathrm{H}]$-nuclear Overhauser enhancement spectroscopy (NOESY).

SITAR triple-resonance experiments

Figure 1(B) shows the pulse sequence of the SITAR HNCA experiment, which is discussed elaborately in the Section on Experimental. Figure 2(A–C) shows the corresponding two-dimensional (2D) SITAR transverse relaxation-optimized spectroscopy (TROSY)-HNCA spectrum of ^{13}C,^{15}N-labeled ubiquitin (2 mM concentration) measured in 10 min with a conventional triple-resonance probe at a magnetic field of 700 MHz ^{1}H-frequency. The 2D SITAR TROSY-HNCA consists of two sub-spectra: the sub-spectrum with the doublet component I^{-}_{24} (Fig. 2(A)) and the complementary sub-spectrum with the component I^{-}_{13} (Fig. 2(B)). The frequency difference between the doublet components of a cross-peak codes the ^{15}N chemical shift as demonstrated for a few examples in Fig. 2(C). The relationship between the frequency difference of the doublet components and the coded ^{15}N chemical shift is given by Eqns (1) or (2). The ^{15}N chemical shift is experimentally determined with an accuracy of ~0.1 ppm[4] (Note, the cryoprobe used here reduces the chemical shift resolution to ~0.4 ppm probably due to the more pronounced B1 inhomogeneity when compared with a conventional probe). The corresponding amide proton chemical shift is measured during acquisition and the sequential and intraresidual $^{13}C^{\alpha}$ chemical shifts are measured in the indirect dimension. Hence, as in the conventional TROSY-HNCA experiment, two cross-peaks for the sequential and intraresidual $^{13}C^{\alpha}$ s are observed for each spin system. Usually, the stronger cross-peaks correspond to intraresidue correlations between the carbons and the ^{15}N–^{1}H moiety, and the weaker cross-peak represents the sequential correlations. In contrast to the conventional TROSY-HNCA spectrum, which is resolved along the ^{15}N dimension by acquiring the ^{15}N chemical shift during the evolution time, the ^{15}N chemical shift in the SITAR TROSY-HNCA experiment is obtained from the chemical shift difference of the two sub-spectra corresponding to the two different spin states.

It is evident that SITAR can also be applied to the amide proton-to-nitrogen-to-alpha-carbon-and-beta-carbon correlation (HNCACB) and the ^{15}N-resolved $[^{1}\mathrm{H},^{1}\mathrm{H}]$-NOESY, although these spectra are much more crowded and complex. The pulse sequences of SITAR-HNCACB and SITAR ^{15}N-resolved $[^{1}\mathrm{H},^{1}\mathrm{H}]$-NOESY experiments are shown in Fig. 1. As an illustration Fig. 2(D) and (E) show parts of the SITAR-HNCACB and SITAR-^{15}N-resolved $[^{1}\mathrm{H},^{1}\mathrm{H}]$-NOESY spectra of ^{13}C,^{15}N-labeled ubiquitin (2 mM concentration) measured with a cryoprobe in 10 min and 1 h, respectively. In general, the concept of SITAR can be applied to all types of triple-resonance experiments including the highly sophisticated HNCACB$^{\mathrm{coded}}$HAHB experiment, which correlates sequential ^{15}N–^{1}H moieties via four probes, the $^{13}C^{\alpha}$, $^{13}C^{\beta}$, $^{1}H^{\alpha}$ and $^{1}H^{\beta}$ chemical shifts.[6,7]

Reconstruction of a 3D spectrum from the pseudo-3D SITAR spectrum by the generation of 3D strips

The principle disadvantage of pseudo-dimensional triple-resonance experiments is the chemical shift degeneracy along the amide proton chemical shift and overlap of peaks due to the lower dimensionality of the spectrum. Indeed, the presence of a large number of peaks in the high-field ^{1}H region of Fig. 2(A–C) is obvious and therefore introduces difficulty to link the vertical connection along $\omega_1(^{13}\mathrm{C})$ dimension for the intraresidual and the sequential cross-peaks of a ^{15}N–^{1}H moiety. In the 3D TROSY-HNCA spectrum, the amide proton chemical shift degeneracy is resolved along the additional ^{15}N dimension and a connection of the intraresidual and sequential cross-peak of a ^{15}N–^{1}H moiety is straightforward, because both are in the same ^{15}N chemical shift-plane and at the same ^{1}H chemical shift. The ^{15}N frequency is also measured in the SITAR TROSY-HNCA using SITAR decoupling which should resolve the apparent ^{1}H chemical shift degeneracy. To resolve the overlap problem to a certain extent as in

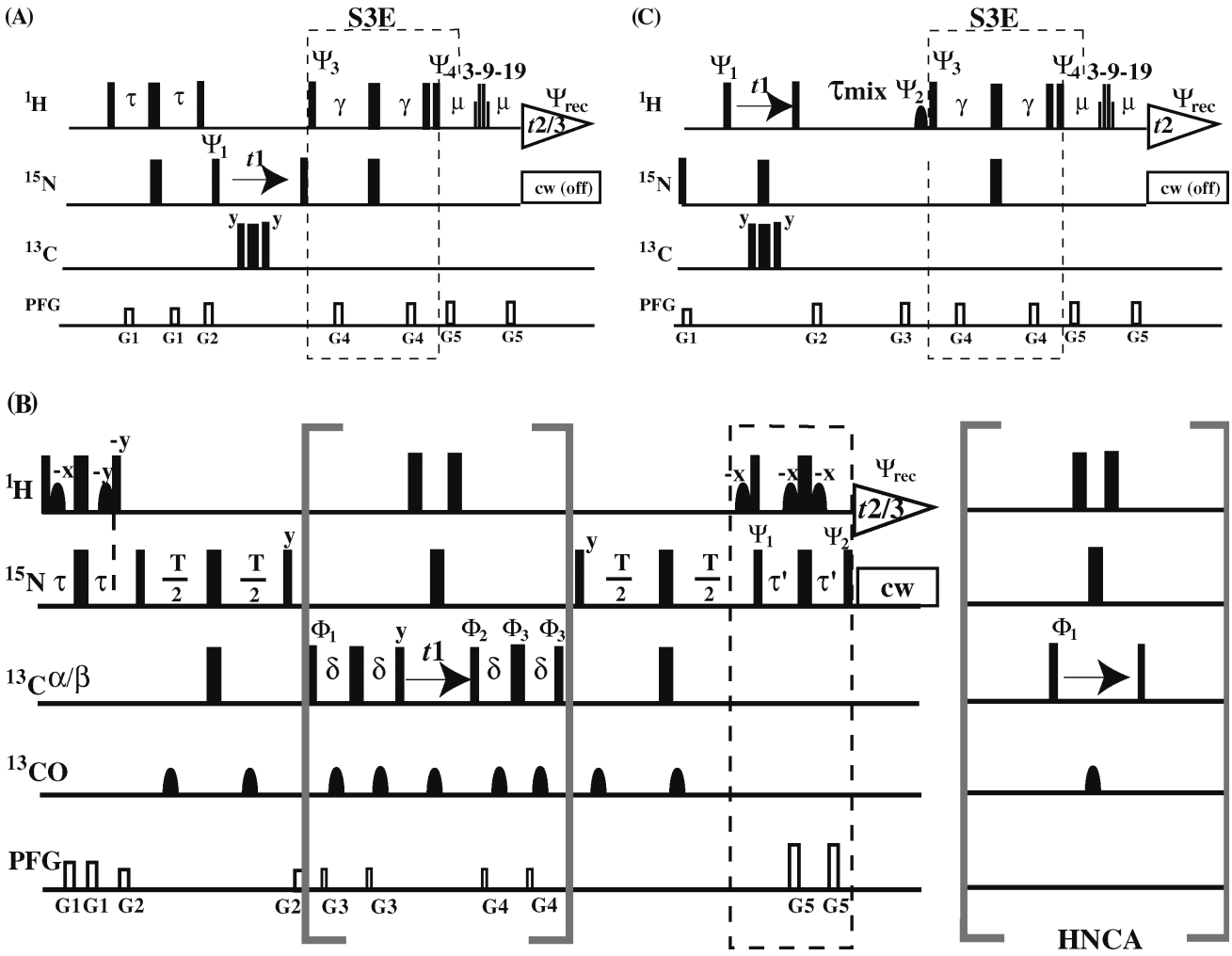

Figure 1. Experimental scheme for the (A) SITAR calibration [^{15}N,^{1}H]-correlation spectrum, (B) SITAR-HNCACB and SITAR-HNCA experiments and (C) SITAR pseudo-3D ^{15}N-resolved [^{1}H,^{1}H]- NOESY for ^{13}C,^{15}N-labeled proteins. The narrow and wide black bars indicate nonselective 90° and 180° pulses, respectively. Off-resonance decoupling on ^{15}N is achieved with a continuous field $\gamma_N B_2/2\pi = 700$ Hz at a frequency $\omega_{cw} = 102$ ppm. (B) The radio-frequency pulses on ^{1}H, ^{15}N, $^{13}C^{\alpha/\beta}$, $^{13}C^{\alpha}$ or $^{13}C'$ were applied at 4.8, 119, 45, 55, and 174 ppm, respectively. On the line marked $^{13}C'$, black sine-bell shapes indicate selective 180° pulses with the duration of 0.08 ms and a Gaussian shape truncated at 5%. The line marked PFG indicates durations and amplitudes of sine shaped pulse magnetic field gradients applied along the *z*-axis. G1: 0.8 ms, 15 G/cm; G2: 0.8 ms, 9 G/cm; G3: 0.5 ms, 18 G/cm; G4: 0.5 ms, 18 G/cm; G5: 0.8 ms, 12 G/cm and G4: 0.8 ms, 22 G/cm. The delays τ, τ', T, δ are 2.7 ms, 2.7−0.5 ms, 24 ms and 3.6 ms, respectively. The phase cycle is $\Psi_1 = \{y + 45°\}$, $\Psi_2 = \{x\}$, $\Phi_1 = \{x, -x\}$, $\Phi_2 = \{-y\}$, $\Phi_3 = \{x\}$, and $\Phi_{rec} = \{y, -y\}$. All other radio-frequency pulses are applied either with phase *x* or as indicated above the pulses. The spin-state selection is achieved by recording of two FID's for each time point with $\Psi_2 = -\Psi_2$ for the second FID, respectively. The two FID's are either added or subtracted and phase corrected by 90° in the acquisition dimension. Quadrature detection in the $^{13}C^{\alpha}(t_2)$ dimension is achieved by the States-TPPI method[8] applied to phase Φ_1, Φ_2 and Φ_3. In the pulse sequence segment within the brackets, the timing of the radio-frequency pulses of the different nuclei have been implemented in a parallel manner to achieve an initial $t_2 = 0$. On the line marked ^{1}H, black sine-bell shapes indicate water-selective 90° pulses with the duration of 1 ms and a Gaussian shape truncated at 5%. With these pulses, the water magnetization stays aligned along the $+z$-axis throughout the experiment ((A) and (C)).[9] The radio-frequency pulses on ^{1}H, ^{15}N, ^{13}C are applied at 4.7, 116 and 110 ppm before the mixing time τ_{mix} and switched to 4.7, 102 and 110 ppm during the mixing time, respectively. On the line marked ^{1}H, black sine-bell shaped pulse indicates a selective 90° pulse with the duration of 1 ms and a Gaussian shape truncated at 5%, which is applied on the water resonance. Also, the pulse train 3−9−19 corresponds to an array of pulses $20.77(x)° - \lambda - 62.21(x)° - \lambda - 131.53(y)° - \lambda - 62.21(x)° - \lambda - 20.77(y)°$ with $\lambda = 150$ μsec.

The following magnetic field gradient pulses are applied along the *z*-axis: G1: 1.0 ms, 13 G/cm; G2: 0.5 ms, 7 G/cm; G3: 1.0 ms, 13 G/cm; G4: 1.0 ms, 13 G/cm; G5: 0.5 ms, 9 G/cm. The delays γ and μ are 1.5 ms and 0.6 ms respectively. τ_{mix} is the NOE mixing time = 80 ms. The phase cycle is $\Psi_1 = \{x, x, -x, -x\}$, $\Psi_2 = -\Psi_3$, $\Psi_3 = \{45°, 225°\}$, $\Psi_4 = \{x\}$ and $\Psi_{rec} = \{-x, x, x, -x\}$. All other radio-frequency pulses are applied either with phase *x* or as indicated above the pulses. Quadrature detection in the $^{1}H(t_1)$ dimension is achieved by the States-TPPI method applied to phase Ψ_1. The spin-state selection is achieved by recording two free induction decays for each time point, with $\Psi_4 = -\Psi_4$ and $\Psi_2 = -\Psi_2$ for the second FID, respectively. The two FID's are either added or subtracted and phase corrected by 90° in the acquisition dimension.

the 3D TROSY-HNCA experiment, a simple algorithm is developed, which is described by Eqn (5) in the Section on Experimental. This algorithm reconstructs from the pseudo-3D SITAR-HNCA sub-spectra, a 3D strip list suppressing crowding of the peaks.

This reconstruction procedure is implemented in the CARA software package.[10] It uses as a starting point the conventional [^{15}N,^{1}H]-correlation spectrum, which correlates for each ^{1}H(j) chemical shift the corresponding ^{15}N(j) chemical shift. The knowledge of the ^{15}N(j) chemical shift and its relationship to $^{R}J(^{1}H,^{15}N)$ expressed in Eqn (2) enables the reconstruction of a 3D strip per ^{15}N–^{1}H moiety. Figure 3(A) shows the [^{15}N,^{1}H]-HMQC together with a SITAR HNCA in the PolyScope tool of CARA. If the user positions the cursor on a cross-peak of the [^{15}N,^{1}H]-HMQC (i.e. HN 38 in Fig. 3(A)), the corresponding SITAR-HNCA 3D strip is simultaneously generated (using Eqns (2) and (5)) and displayed on the right side of the PolyScope window (see Fig. 3(A)). For most of the spin systems the $^{13}C^{\alpha}(i)/^{13}C^{\alpha}(i-1)$ pair can immediately be recognized and picked. This procedure is identical to the conventional procedure with triple-resonance experiments. Hence, the user does not even realize that a projected spectrum is displayed. However, a lower resolution of ~2 ppm along the ^{15}N dimension in the reconstructed 3D strip (see Section on Experimental) is recognizable, which is in contrast to the ~0.4 ppm resolution of the conventional 3D

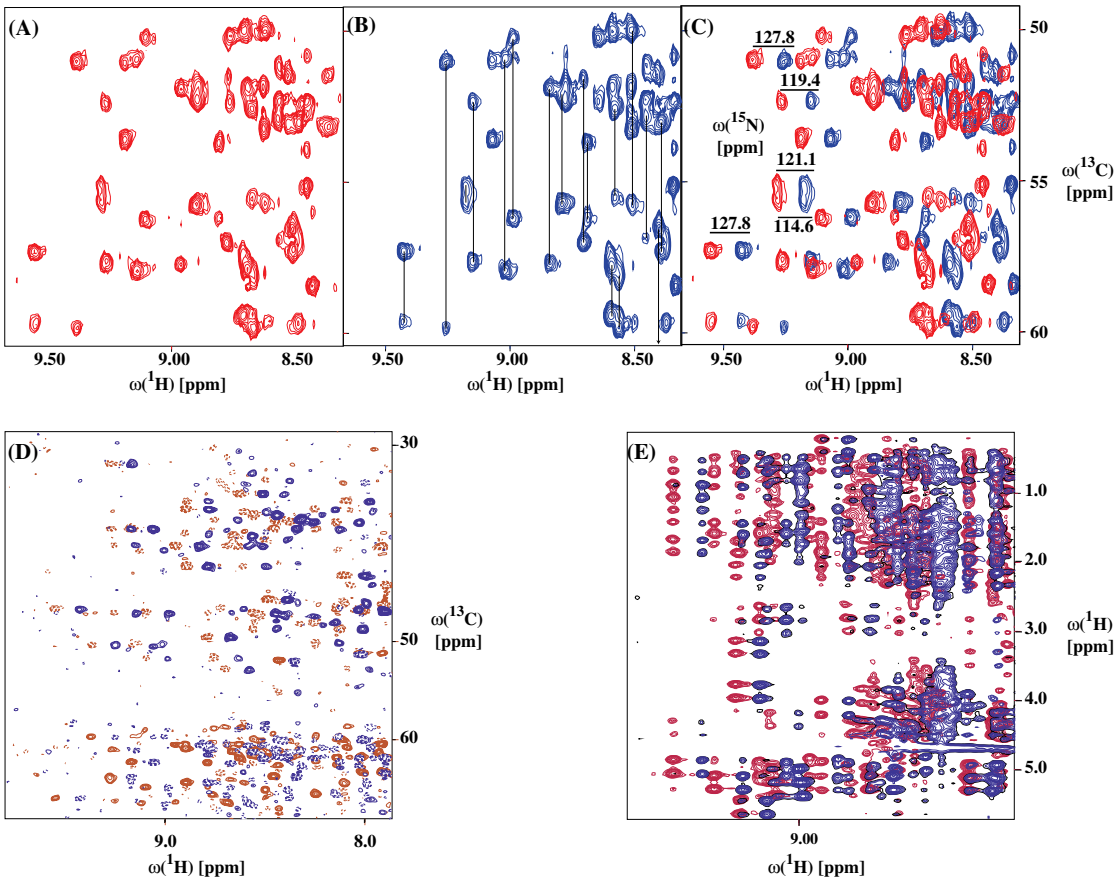

Figure 2. Pseudo-3D (A–C) SITAR-HNCA, (D) SITAR-HNCACB and (E) SITAR ^{15}N-resolved [^{1}H,^{1}H]-NOESY spectra of ^{13}C,^{15}N-labeled ubiquitin. Red contour lines correspond to the sub-spectrum with the component I_{24}^{-} and blue lines correspond to the complementary sub-spectrum with the component I_{13}^{-} of the doublet. Superposition of both sub-spectra is shown in (C–E). The SITAR-HNCA experiment was recorded at 20 °C with a 2 mM sample of ^{13}C,^{15}N-labeled ubiquitin in a mixed solvent of 95% H_2O/5% D_2O at pH 7, using a Bruker Avance 700 MHz spectrometer equipped with five radio-frequency channels, a pulsed field gradient unit and a conventional triple-resonance probe with an actively shielded z-gradient coil. The following parameter settings were used: data size $= 2 * 50(t_1) * 2048(t_2)$ complex points; $t_{1\,max}$ (^{13}C) = 8 ms, $t_{2\,max}$ (^{1}H) = 200 ms. The data set was zero-filled to 256 * 8192 complex points; eight scans per increment were acquired, resulting in 10 min of measuring time. (D) The SITAR-HNCACB experiment was recorded at 20 °C with a 2 mM sample of ^{13}C,^{15}N-labeled ubiquitin in a mixed solvent of 95% H_2O/5% D_2O at pH 7, using a Bruker Avance 700 MHz spectrometer equipped with five radio-frequency channels, a pulsed field gradient unit and a cryoprobe with an actively shielded z-gradient coil. The following parameter settings were used: data size $= 2 * 80(t_1) * 1024(t_2)$ complex points; $t_{1\,max}$ (^{13}C) = 7 ms, $t_{2\,max}$ (^{1}H) = 100 ms. The data set was zero-filled to 256 * 8192 complex points; four scans per increment were acquired, resulting in 10 min of measuring time. (E) The ^{15}N-resolved [^{1}H,^{1}H]-NOESY spectra was measured with the identical set up as the SITAR-HNCACB. The following parameter settings were used: data size $= 2 * 400(t_1) * 1024(t_2)$ complex points; $t_{1\,max}$ (^{1}H) = 40 ms, $t_{2\,max}$ (^{1}H) = 100 ms. The data set was zero-filled to 1024 * 8192 complex points; eight scans per increment were acquired, resulting in 1 h of measuring time. The use of a strong window function along t_2 enhances the resolution along both $\omega(^{1}H)$ and $\omega(^{15}N)$, respectively.

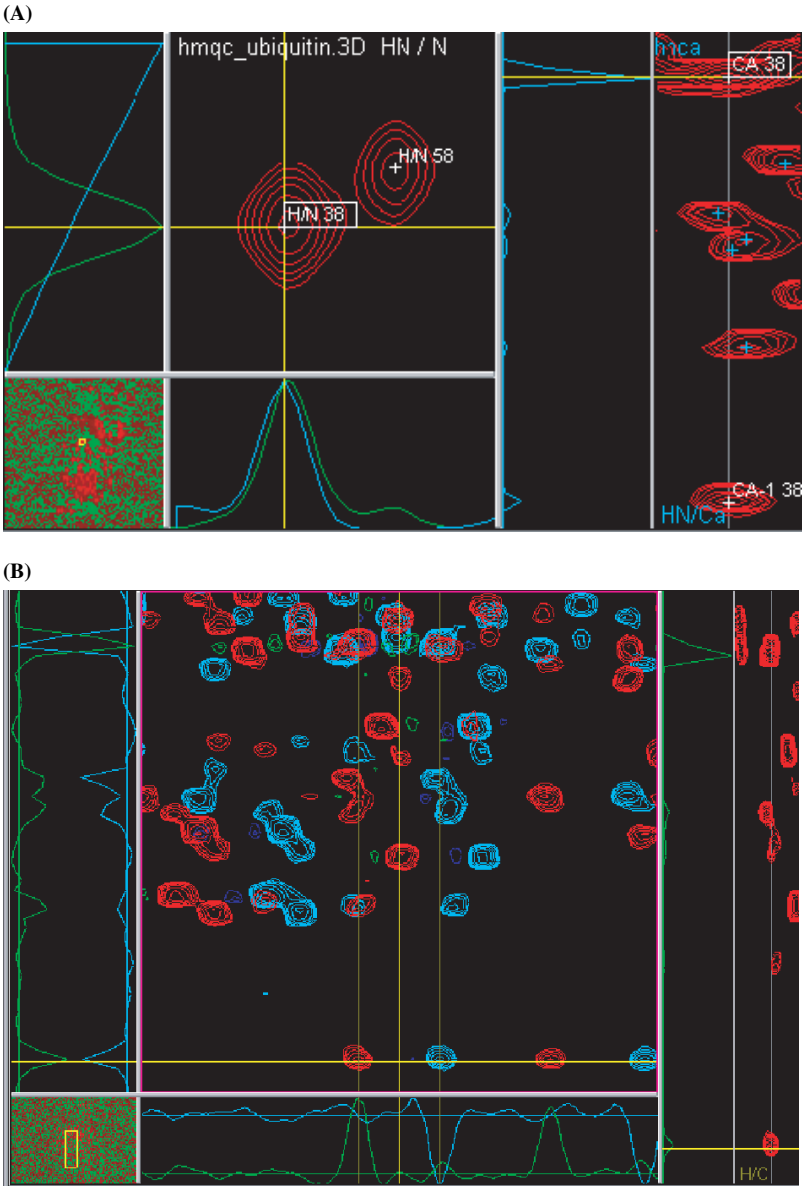

Figure 3. (A) PolyScope presentation and (B) SitarViewer presentation of SITAR-HNCA. (A) Magnification of the cross-peak $^{15}N/^{1}H$ 38 of the [^{15}N,^{1}H]-HMQC spectrum (shown on the lower left of the PolyScope) is shown. The cursor positioning on top of the cross-peak generates its corresponding 3D strip of the SITAR-HNCA on the right side of the PolyScope by using the reconstruction algorithm of Eqn (5). The cross-peaks in the strip have been assigned accordingly. (B) Superposition of the two SITAR-HNCA sub-spectra (I^{-}_{24} shown in red, and I^{-}_{13} shown in cyan) is shown for the spin system 38. The lines are set to measure the residual scalar coupling between the two doublet components (also referred as twin peaks in the text), which is then transferred to a ^{15}N chemical shift and concomitantly generates a 3D strip shown on the right side of the SitarViewer.

triple-resonance experiment, and generates therefore more ambiguities.

To resolve these ambiguities a dedicated tool 'SitarViewer' has been implemented in CARA, which enables the analysis of the SITAR-HNCA spectra in an E. COSY-manner. The SitarViewer works quite similar to the other scope windows of CARA (e.g. cursor navigation, scrolling or zooming). Figure 3(B) shows part of the SITAR-HNCA spectrum in SitarViewer. The middle panel displays the two sub-spectra I^{-}_{24} (red) and I^{-}_{13} (cyan) as an overlay (for an easy analysis SitarViewer also allows to quickly show or hide the two sub-spectra). A typical $^{13}C^{\alpha}(i)/^{13}C^{\alpha}$ $(i-1)$ twin pair of cross-peaks are visible along the ^{13}C frequency axis at the split cursor positions. The two doublet components form a characteristic pattern, which can be recognized quite well, even in crowded areas of the spectrum. The resulting reconstructed 3D strip is displayed at the right side of the scope (see Fig. 3(B)). Using SitarViewer a resolution of ~0.4 ppm along the ^{15}N-dimension is obtained.

To connect the two assignment tools, the option *View/Sync to Global Cursor* in PolyScope is established. With the option 'on' a change of the cursor position (either on 2D plane or 3D strip) is immediately reflected in the SitarViewer. Cursor movement along the Y axis (^{15}N dimension) of the [^{15}N,^{1}H]-HMQC immediately adjusts the difference in the splitting designated by the cursors in the SitarViewer. On

the other hand, if the difference in the splitting is directly changed in SitarViewer (either by SHIFT-dragging the mouse or by pressing the cursor keys together with the SHIFT key), the ^{15}N dimension of the cursor in PolyScope is updated accordingly. This allows for two kinds of assignment strategies, either using PolyScope or for higher resolution along ^{15}N dimension using SitarViewer. More details and practical aspects of preparation, configuration and assignment of SITAR-spectra in CARA are given in the Supplementary Material.

Sequential assignment with the SITAR spectra

Once spin systems have been identified, the combination of spin systems to fragments and the alignment of them to the amino acid sequence can be done similar to the conventional triple-resonance spectra. Hence, the dedicated scopes and the tools of CARA can be applied to the SITAR spectra for this purpose. This includes the backbone assignment automation algorithms AutoLink,[11] which was developed using the scripting language and the conceptual model of CARA. As an illustration, Fig. 4 shows several aligned and assigned strips of the SITAR-HNCA of ubiquitin in StripScope. The assigned spins of this system are listed in the left part of the figure. Similarly, SITAR-HNCACB strips or strips of the SITAR-^{15}N-resolved [^{1}H,^{1}H]-NOESY of the same fragment can be displayed.

DISCUSSION

The combination of SITAR with the proposed 3D reconstruction-algorithm and its implementation in the software CARA enables the generation of 3D strip lists of triple-resonance experiments and ^{15}N-resolved [^{1}H,^{1}H]-NOESY experiments. SITAR pseudo-3D spectra are easily analyzed and established software packages for conventional 3D experiments can be utilized. This reconstruction of a 3D spectrum measured by pseudo-3D experiments enable the collection of highly resolved spectra in several minutes without the drawback of peak crowding and chemical shift degeneracy. SITAR pseudo-3D spectroscopy is therefore an excellent technique for applications in the 'non-sensitivity-limited' data collection regime for well structured small and medium size proteins. Its short acquisition time classifies SITAR to the group of 'fast multidimensional NMR experiments'. We conclude that SITAR spectroscopy is superior to the other three proposed techniques of fast multidimensional NMR for the following reasons: (i) Multidimensional Hadamard spectroscopy needs prior knowledge of the chemical shift frequencies of interest,[3] which is not a prerequisite for the SITAR-technology. (ii) In GFT spectroscopy[2] the intrinsic overlap problem of pseudo-dimensional spectroscopy is also resolved by two sub-spectra. However, with GFT spectroscopy manual assignment is not straightforward, because the sequential cross-peaks of residue i do not align in the indirect dimension with the intraresidual cross-peaks of residue $i-1$ due to parallel evolutions of ^{13}C and ^{15}N. Hence, GFT spectroscopy asks for cross-peak-derived chemical shift list-based assignment strategies rather than the use of 3D strips.[12,13] This is in striking contrast to the SITAR-technology, in which the reconstruction of the 3D spectrum facilitates the (manual) assignment procedure and enables the application of established assignment strategies and software packages, which use the spectrum for the assignment process. Furthermore, since no chemical shift evolution is needed to detect the ^{15}N chemical shift, the reconstructed SITAR 3D spectrum has the sensitivity of a 2D spectrum and is therefore a factor of 2 more sensitive than its GFT analog (e.g. SITAR-HNCA and (3,2)-HNCA, respectively). (iii) The 3D projection spectroscopy[1,14] also reconstructs the 3D spectrum. However, 3D projection spectroscopy cannot be applied straightaway to the ^{15}N-resolved [^{1}H,^{1}H]-NOESY experiment due to the large amount of NOE cross-peaks expected per ^{15}N,^{1}H-moiety (Fig. 2(D)). Furthermore, it is also a factor of $2^{0.5}$ less sensitive than its SITAR counterpart.

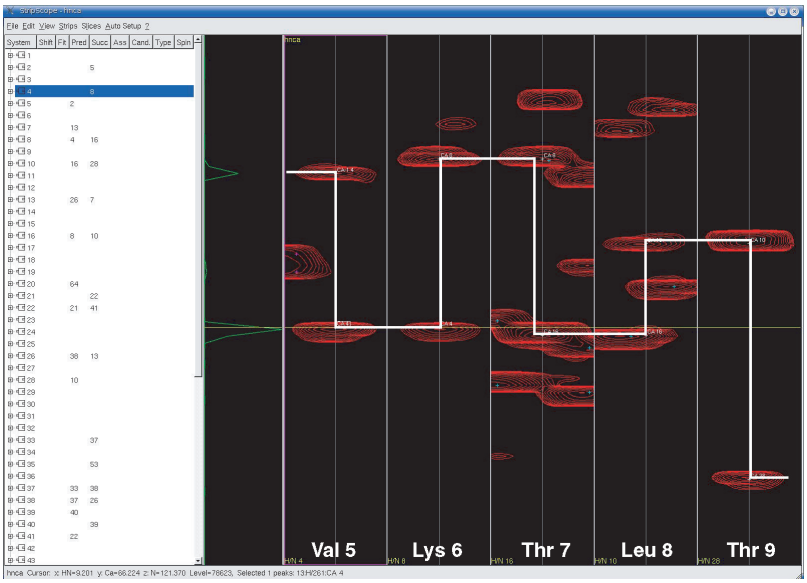

Figure 4. SITAR-HNCA strip fragment of residues 5–9 of ^{13}C,^{15}N-labeled ubiquitin shown in StripScope.

A potential disadvantage of SITAR-based triple-resonance experiments is that off-resonance decoupling is influenced by B1 inhomogeneity and requires an initial calibration of the relationship between residual scalar coupling and chemical shift. Furthermore, SITAR is a chemical shift detection method different from the well-established time evolution and requests therefore an additional activation energy of the NMR spectroscopist in order to be used.

CONCLUSION

The proposed SITAR spectroscopy in conjunction with the software package presented enables the measurement of multidimensional triple-resonance experiments and NOESY experiments with high resolution in only minutes. It is, however, obvious that this technique including the other proposed techniques for fast multidimensional NMR are advantageous only for small well-behaved proteins. For larger proteins, we propose the use of the recently developed TROSY-HNCA^{coded}CO and TROSY-HNCA^{coded}CB experiments,[7,15] which are trimmed for high sensitivity in combination with large information content.

EXPERIMENTAL

Experimental relation between $^{R}J(^{1}H,^{15}N)$ and ^{15}N chemical shift by the SITAR [^{15}N,^{1}H]-correlation spectrum

From Eqn (1) it can be seen, that SITAR is based on a specific relation between the residual scalar coupling $^{R}J(^{1}H,^{15}N)$ and the chemical shift of spin ^{15}N. Since all components of this relation are known ($^{1}J(^{1}H,^{15}N) = -92$ Hz) and given the experimental parameters (i.e. $\omega_{cw} = 102$ ppm and $\gamma_N B_2/2\pi$ of 685 Hz), the relationship can be calculated. In order to calibrate accurately this relationship, the measurement of a modified 2D [$^{15}N-^{1}H$]-correlation experiment is recommended (Fig. 1(A)). In this experiment, a S3E element[16] is added prior to acquisition and off-resonance decoupling is applied on ^{15}N during acquisition with identical experimental parameters as the triple-resonance experiments. The resulting two sub-spectra yield the chemical shifts of ^{1}H and ^{15}N and the corresponding $^{R}J(^{1}H,^{15}N)$ per $^{1}H,^{15}N-$moiety and allows the experimental extraction of $\gamma_N B_2/2\pi$ which in the example given turned out to be 700 Hz rather than the calculated 685 Hz (Note: this difference is not substantial for the reconstruction of the 3D strip list). These spectra are therefore used to calibrate the pseudo-dimension and play the mediator between a conventional [^{15}N,^{1}H] correlation spectrum and the SITAR triple-resonance experiments and ^{15}N-resolved [^{1}H,^{1}H]-NOESY experiments. The values of $\gamma_N B_2/2\pi$,[1] $J(^{1}H,^{15}N)$ and ω_{cw} are required by the software package CARA in order to use SITAR (see below).

SITAR applied to pseudo-3D triple-resonance experiments

The proposed SITAR-TROSY-HNCA and SITAR-TROSY-HNCACB experiments are essentially the pseudo-3D versions of the corresponding TROSY-HNCA and 3D TROSY-HNCACB[17,18] experiments (Fig. 1). Magnetization is transferred from ^{1}H via ^{15}N to $^{13}C^{\alpha/\beta}$. During the frequency labeling period t_1 the $^{13}C^{\alpha/\beta}$ chemical shifts evolve. After t_1, magnetization is transferred back to ^{15}N and finally back to ^{1}H with a spin-state selection element[16,18,19] depicted in Fig. 1(B). During ^{1}H acquisition off-resonance decoupling is applied to detect the ^{15}N chemical shift.[4] The spin states are selected by the addition or subtraction of two alternate FIDs with pulse sequences that differ by the sign of phase Ψ_2 (the sub-spectrum with the I^{-}_{13} component is 90° out of phase). The chemical shift of the ^{15}N attached to ^{1}H is determined, by measuring the difference between the doublet components and using Eqn (1). The flow of coherence for the SITAR-TROSY-HNCACB is described as follows:

$$^{1}H(i) \rightarrow {}^{15}N(i) \begin{matrix} \nearrow {}^{13}C^{\alpha}(i)[t1] \\ \rightarrow {}^{13}C^{\beta}(i)[t1] \\ \rightarrow {}^{13}C^{\alpha}(i\text{-}1)[t1] \\ \searrow {}^{13}C^{\beta}(i\text{-}1)[t1] \end{matrix} \rightarrow {}^{15}N(i) \begin{matrix} \nearrow {}^{1}H(i)\ \exp[\mathbf{i}\ \{\omega(H(i)) \\ \searrow -\pi\ {}^{R}J({}^{15}N(i),{}^{1}H(i))\}\ t2] \end{matrix}$$

where t_1 is the ^{13}C evolution time and t_2 is the ^{1}H acquisition time. Indices i and $i-1$ indicate that coherence is transferred from $^{15}N(i)-^{1}H(i)$ to both the sequentially and the intraresidually adjoining carbons. The coded $^{15}N(i)$ chemical shift is designated in the residual scalar coupling $^{R}J(^{15}N(i),^{1}H(i))$, which can be extracted from the two sub-spectra containing either the I^{-}_{24} or I^{-}_{13} component. The relationship between the $^{15}N(i)$ chemical shift and $^{R}J(^{15}N(i),^{1}H(i))$ is given by Eqn (1). The coherence flow for the SITAR-TROSY-HNCA is similar, but lacks the $^{13}C^{\beta}$ chemical shift evolution.

SITAR applied to pseudo-3D ^{15}N-resolved [^{1}H,^{1}H]-NOESY experiment

The concept of SITAR is incorporated into the 2D [^{1}H,^{1}H]-NOESY experiment for identifying dipolar coupled proton pairs $^{1}H(i)$ and $^{1}H(j)$ by their chemical shifts and the chemical shifts of the attached hetero-nuclei $^{15}N(j)$ (Fig. 1(C)). The two frequencies of the coupled protons $\omega(^{1}H(i))$ and $\omega(^{1}H(j))$ are determined during t_1 and t_2, respectively. The heteronuclear frequency $\omega(^{15}N(j))$ is obtained by applying SITAR during the acquisition time using the spin-state selection element[16] depicted in Fig. 1(C) and off-resonance decoupling as described by Grace and Riek.[4] The spin states are selected by the addition or subtraction of two alternate FIDs with pulse sequences that differ by the sign of phase Ψ_2 (the sub-spectrum with the I^{-}_{13} component is 90° out of phase). The chemical shift of the ^{15}N attached to the ^{1}H is coded in the residual scalar coupling through Eqn (1). In summary, the coherence flow can thus be described as:

$$^{1}H(i)\ [t1] \xrightarrow{NOE} \begin{matrix} \nearrow {}^{1}H(j)\ \exp[\mathbf{i}\ \{\omega({}^{1}H(j)) + \pi\ {}^{R}J({}^{15}N(j),{}^{1}H(j))\}\ t2] \\ \searrow {}^{1}H(j)\ \exp[\mathbf{i}\ \{\omega({}^{1}H(j)) - \pi\ {}^{R}J({}^{15}N(j),{}^{1}H(j))\}\ t2] \end{matrix}$$

where t_1 is the evolution time of $^{1}H(i)$ and t_2 is the acquisition time during which $^{1}H(j)$ evolves.

SITAR projection and reconstruction into a 3D spectrum

As mentioned above, a SITAR triple-resonance experiment corresponds to a projection of the 3D $^{1}H-^{15}N-^{13}C$ spectrum onto a pair of two-dimensional $^{1}H-^{13}C$ sub-spectra

designated I^{-}_{24} and I^{-}_{13}, because they contain the corresponding multiplet components $I^{-}_{24} = \omega(^1\mathrm{H}) + {}^{R}J(^{15}\mathrm{N},^1\mathrm{H})$ and $I^{-}_{13} = \omega(^1\mathrm{H}) - {}^{R}J(^{15}\mathrm{N},^1\mathrm{H})$, respectively. The ^{15}N dimension is therefore encoded by the residual scalar coupling in the ^{1}H dimension given by,

$$ {}^{R}J(^1\mathrm{H},^{15}\mathrm{N}) = {}^{1}J(^1\mathrm{H},^{15}\mathrm{N})|\omega_\mathrm{N} - \omega_\mathrm{cw}|/[(\gamma_\mathrm{N}B_2/2\pi)^2 + (\omega_\mathrm{N} - \omega_\mathrm{cw})^2]^{0.5} \quad (2) $$

and each ^{1}H–^{15}N–^{13}C cross-peak is projected onto a pair of I^{-}_{24}-C and I^{-}_{13}-C doublet peaks around $\omega(^1\mathrm{H})$ following Eqn (2).

Knowing the frequencies $\omega(^1\mathrm{H})$ and $\omega(^{15}\mathrm{N})$ from a cross-peak in the [^{15}N,^{1}H]-HMQC spectrum, its counter part in the 3D spectrum can be efficiently reconstructed from the SITAR spectra by multiplying the intensities of the I^{-}_{24} and I^{-}_{13} spectra at a given frequency $\omega(^1\mathrm{H})$ with the calculated offset $o = {}^{R}J(^1\mathrm{H},^{15}\mathrm{N})/\Delta$, where Δ corresponds to the chemical shift difference between two adjacent points of the ^{1}H dimension of the spectrum reflecting the spectral resolution. If $a_{L,R}(i)$ are the amplitudes of the ith spectrum point along the ^{1}H dimension of the I^{-}_{24} and I^{-}_{13} sub-spectra at a given ^{13}C chemical shift and a_max is the maximum amplitude found in either of the two projections, $a(i)$ of the reconstructed 3D spectrum is given by:

$$ a(i) = a_L(i-o)\cdot a_R(i+o)\cdot\lambda(i)/\sqrt{a_\mathrm{max}} \quad (3) $$

In Eqn (5) it is assumed that I^{-}_{24} and I^{-}_{13} projections have the same polarity (if not, $a_{L,R}(i)$ is multiplied by ±1). The function $\lambda(i) = m(i)\cdot c(i) = [0,1]$ is used as a filter to reduce artifacts and to increase reconstruction quality. The optional clipping part $c(i)$ is used to get rid of negative amplitudes, and is given by,

$$ c(i) = \begin{cases} 1, & a_L(i) > 0 \wedge a_R(i) > 0 \\ 0, & \text{else} \end{cases} \quad (4) $$

Equation (6) is used for SITAR spectrum-types with homogeneous polarity over the whole spectrum, e.g. SITAR-HNCA.

$$ c(i) = \begin{cases} 1, & a_L(i) > 0 \wedge a_R(i) > 0 \vee a_L(i) < 0 \wedge a_R(i) < 0 \\ 0, & \text{else} \end{cases} \quad (5) $$

Equation (7) is less restrictive and therefore suited for SITAR spectrum-types with mixed peak polarity, e.g. SITAR-HNCACB, where the $^{13}C^{\alpha}(i)$ and $^{13}C^{\alpha}(i-1)$ cross-peaks have positive amplitude and the $^{13}C^{\beta}(i)$ and $^{13}C^{\beta}(i-1)$ cross-peaks are negative, respectively.

The optional *gradient matching* term $m(i)$ can be seen as a correspondence measure of the amplitude envelope gradient at $a_L(i-o)$ and $a_R(i-o)$.

$$ m(i) = 1 - (\arctan(a_L(i-o) - a_L(i-o-1)) - \arctan(a_R(i+o+1) - a_R(i+o))/\pi \quad (6) $$

The importance of the gradient matching term in increasing the chemical shift resolution along the reconstructed ^{15}N dimension is shown in Fig. 5. Only in the presence of the gradient matching term, a reasonable resolution of ~2 ppm is obtained. Note, that this chemical shift resolution obtained by the algorithm of Eqn (5) is much lower than the resolution obtained by analyzing the spectra by measuring ${}^{R}J(^1\mathrm{H},^{15}\mathrm{N})$ in an E. COSY-manner. In crowded regions of the spectrum, it is therefore of advantage to generate the strip by analyzing the spectra in an E. COSY-manner. For this situation, a special routine called SitarViewer has been developed within the software package CARA (see above).

SITAR implementation in CARA

CARA is a well-established resonance assignment software package developed at the Institute of Molecular Biology and Biophysics at ETH Zurich. The free software can be downloaded from http://www.nmr.ch. A detailed description of

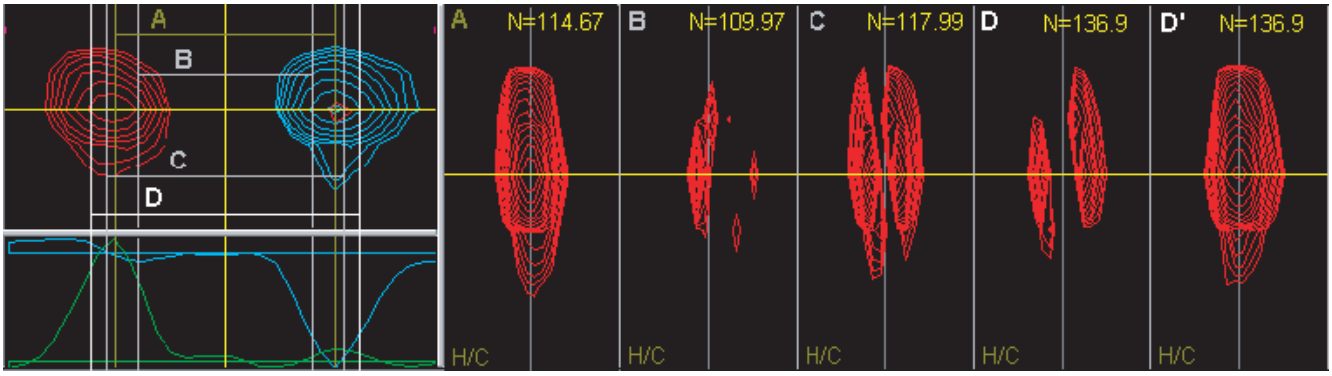

Figure 5. Reconstruction of a HNCA 3D strip from the Pseudo-3D SITAR-HNCA spectrum using the algorithm of Eqn (5). On the top left, a superposition of the two SITAR-HNCA sub-spectra (I^{-}_{24} shown in red, and I^{-}_{13} shown in cyan) is shown for one of the spin system. The lines designated by (A–D) are measuring the residual scalar coupling between the two doublet components, which is then transferred to a ^{15}N chemical shift and concomitantly generates a 3D strip shown in the boxes (A–D). Only the lines designated by A are correctly measuring the residual scalar coupling and are therefore generating a strip with the corresponding cross-peak. In contrast, lines designated by (B–D) do not reconstruct correctly the 3D strip and its cross-peak as shown in the boxes (B–D). The strip D′ shows the reconstruction of the strip in the absence of the use of the *gradient matching* term, which reduces the resolution dramatically.

Table 1. SITAR configuration file in CARA

Name	Value	Description
lhp	File name	The name of the file containing the 2D left-hand projection spectrum designated I^{-}_{24}. All spectrum formats supported by CARA can be used.
rhp	File name	The name of the file containing the 2D left-hand projection spectrum designated I^{-}_{13}. All spectrum formats supported by CARA can be used.
j	Hz	Scalar coupling used to code the SITAR frequency (e.g. $^1J(^1H,^{15}N)$)
rf	MHz	The spectrometer frequency of the projected dimension (e.g. $\omega(^{15}N)$)
cw	ppm	Off-resonance decoupling frequency (e.g. $\omega_{cw} = 102$ ppm)
c	Number (Hz?)	Decoupling power of the off-resonance decoupling (e.g. $\gamma_N B_2/2\pi = 700$ Hz)
sc	Number	Number of virtual frequency points along the projected dimension. Half of the number along the direct dimension of lhp is used as default.
sw	ppm	Spectral width along the projected dimension. A spectral width corresponding to 0.98 * j is used as default.
dir	'asc'|'desc'	Controls, how cw is interpreted. With 'asc' (the default) the ppm scale of the projected dimension runs from cw + sw to cw. With 'desc' it runs in the opposite direction from cw to cw − sw.
lpol	'pos'|'neg'	The polarity of the lhp projection spectrum. Default is 'pos'.
rpol	'pos'|'neg'	The polarity of the rhp projection spectrum. Default is 'neg'.
Matchgrad	'yes'|'no'	Used to switch on or off the gradient matching feature (Eqn (6)). Default is 'on'.
Interpolate	'yes'|'no'	If 'yes', the ^{15}N offset is linearly interpolated between the defined frequency points. Default is 'yes'.
Rectify	'yes'|'no'	If 'yes', clipping according to Eqn (5) is applied. Default is 'yes'.
Clip	'yes'|'no'	If 'yes', clipping according to Eqn (4) is applied. Default is 'yes'.
lbl	String	An optional label for the projected dimension.

the software can be found in Ref. 10, 20. CARA handles the SITAR spectra including the 3D reconstruction-algorithm described above. SITAR spectra can be loaded in CARA-like ordinary 3D spectra. Thus, all scope windows provided by CARA for triple-resonance analysis can also be used for SITAR spectra.

The SITAR file format is implemented by means of a configuration file pointing to two standard 2D spectra. CARA expects the configuration file to have a file extension of the form '*.sitar'. The configuration file contains lines of ASCII text, each representing a name-value pair listed in Table 1. It includes the name of the two SITAR sub-spectra (rhp and lhp for right-hand projection and left-hand projection, which stands for the sub-spectra I^{-}_{24} and I^{-}_{13}, respectively), the scalar coupling (*j*) used to code the SITAR frequency (rf), the off-resonance decoupling frequency (cw), and the decoupling power (c). The following box gives an example of a SITAR-HNCA configuration file used in this publication:

```
rhp=sitar_hncaI13.3D.param
lhp=sitar_hncaI24.3D.param
j=92
rf=70.95
cw=102
c=700
lpol=pos
rpol=neg
matchgrad=yes
```

The SITAR configuration file format can be used for different kinds of SITAR spectrum-types (e.g. HNCA, HNCACB, ^{15}N-resolved [^1H,^1H]-NOESY, etc.). The lhp and rhp spectra are required to have the same number of dimensions and corresponding dimension types. The current implementation in CARA only supports 2D projection spectra (i.e. pseudo-3D SITAR spectra).

Supplementary material

Supplementary electronic material for this paper is available in Wiley InterScience at: http://www.interscience.wiley.com/jpages/0749-1581/suppmat/

Acknowledgement

RR is a Pew Scholar. The work has been supported in part by the NIH.

REFERENCES

1. Freeman R, Kupce E. *J. Biomol. NMR* 2003; **27**: 101.
2. Kim S, Szperski T. *J. Am. Chem. Soc.* 2003; **125**: 1385.
3. Kupce E, Freeman R. *J. Biomol. NMR* 2003; **25**: 349.
4. Grace CRR, Riek R. *J. Am. Chem. Soc.* 2003; **125**: 16104.
5. Freeman R. *A Handbook of Nuclear Magnetic Resonance*. Longman Scientific & Technical: Essex: 1988.
6. Pegan S, Kwiatkwoski W, Choe S, Riek R. *J. Magn. Reson.* 2003; **165**: 315.
7. Kwiatkwoski W, Riek R. *J. Biomol. NMR* 2003; **25**: 281.
8. Marion D, Ikura M, Tschudin R, Bax A. *J. Magn. Reson.* 1989; **85**: 393.
9. Grzesiek S, Bax A. *J. Am. Chem. Soc.* 1993; **115**: 12593.
10. Keller R. *The computer aided resonance assignment tutorial*, ISBN 3-85600-112-3. Cantina Verlag: Goldau, 2004.
11. Masse J, Keller R. *J. Magn. Reson.* 2005; **174**: 133.

12. Bartels C, Xia T, Billeter M, Guntert P, Wuthrich K. *J. Biomol. NMR* 1995; **6**: 1.
13. Moseley HN, Riaz N, Aramini JM, Szyperski T, Montelione GT. *J. Magn. Reson.* 2004; **170**: 263.
14. Kupce E, Freeman R. *J. Am. Chem. Soc.* 2004; **126**: 329.
15. Ritter C, Luhrs T, Kwiatkwoski W, Riek R. *J. Biomol. NMR* 2003; **28**: 289.
16. Meissner A, Duus J, Sørensen OW. *J. Magn. Reson.* 1997; **128**: 92.
17. Salzmann M, Wider G, Pervushin K, Senn H, Wuthrich K. *J. Am. Chem. Soc.* 1999; **121**: 844.
18. Pervushin K, Riek R, Wider G, Wüthrich K. *Proc. Natl. Acad. Sci. U.S.A.* 1997; **94**: 12366.
19. Sørensen MD, Meissner A, Sørensen OW. *J. Magn. Reson.* 1999; **137**: 237.
20. Keller R. *Optimizing the Process of Nuclear Magnetic Spectrum Analysis and Computer Aided Resonance Assignment*,Dissertation Nr. 15947 of the Swiss Federal Institute of Technology: Zurich, 2005.